ANTICANCER RESEARCH *41*: 6013-6021 (2021)
doi:10.21873/anticanres.15420

The Thioredoxin-1 Inhibitor, PX-12, Suppresses Local Osteosarcoma Progression

HIDEYUKI KINOSHITA[1], OSAMU SHIMOZATO[2], TAKESHI ISHII[1], HIROTO KAMODA[1], YOKO HAGIWARA[1], SEIJI OHTORI[3] and TSUKASA YONEMOTO[1]

[1]*Department of Orthopedic Surgery, Chiba Cancer Center, Chiba, Japan;*
[2]*Laboratory of Oncogenomics, Chiba Cancer Center Research Institute, Chiba, Japan;*
[3]*Department of Orthopedic Surgery, Graduate School of Medicine, Chiba University, Chiba, Japan*

Abstract. *Background/Aim: The thioredoxin-1 (Trx-1) inhibitor, PX-12, is active against several cancer types. This study aimed to evaluate its effects on local osteosarcoma (OS) progression and to describe PX-12-related signal transduction pathways. Materials and Methods: Publicly available expression cohort data were analyzed to determine the relationship between the expression levels of TXN, which codes for the Trx protein, and survival in patients with OS. Murine LM8 OS cells were stimulated with PX-12. Apoptosis-related protein levels, cell viability, caspase activity, and wound healing were evaluated. PX-12 efficacy in suppressing tumor progression was evaluated in C3H mice injected with LM8 cells. Results: High TXN expression was a negative prognostic factor for metastasis and overall survival in OS patients. PX-12 induced apoptosis in OS cells via the oxidative stress-MAPK-caspase 3 pathway and suppressed OS cell migration. PX-12 suppressed local OS progression. Conclusion: PX-12 is a potential therapeutic agent for use in suppressing local OS progression.*

Osteosarcoma (OS) is an extremely rare malignant tumor with a high incidence rate in adolescents and young adults, and is associated with poor survival. Surgery and perioperative chemotherapy are used for OS treatment (1). Standard chemotherapy for pediatric patients involves the use of cisplatin, doxorubicin, and high-dose methotrexate. However, the five-year survival probability in OS patients is poor, especially in those with local progression of the disease, chemotherapy resistance, or metastases. At present, chemotherapeutic agents used in treating OS include conventional cytotoxic agents, which have serious side effects; therefore, the development of novel therapeutic agents is desirable.

The oxidation-reduction (redox) system regulates various essential metabolic functions of the cell. Thioredoxin (Trx) and Trx reductases (TrxR), which are key molecules of the redox system, function as reactive oxygen species (ROS) scavengers, and are associated with the development of several diseases, including cancers (2). ROS have been reported to activate mitogen-activated protein kinases (MAPKs), such as c-Jun N-terminal kinase (JNK) and p38, thereby inducing apoptosis in cancer cells (3). Recently, we reported that auranofin (AUR), a TrxR inhibitor, significantly inhibited pulmonary OS metastasis *in vivo*, indicating that the redox system, which includes Trx and TrxR, could be a potential therapeutic target for OS treatment (4). PX-12, an irreversible Trx-1 inhibitor, has been shown to be a potential therapeutic agent for the treatment of several cancer types (5). However, no studies have evaluated the effects of PX-12 on various sarcomas, including OS. Therefore, we aimed to investigate the effects of PX-12 on local OS progression and to describe its related signal transduction pathways.

Materials and Methods

Bioinformatics. The Trx protein is encoded by *TXN* (6). We investigated the relationship between *TXN* (ILMN_1680314) expression and disease outcome in OS patients using public microarray data (GSE42352). *TXN* expression data were downloaded from the R2 microarray analysis and visualization platform, and the R2-based software was used to draw Kaplan–Meier survival curves. As described in a previous study (4), the best cut-off value for the survival analysis was determined as the expression value obtained when the statistic log-rank for the separation of the survival curves reached its highest level.

Antibodies and reagents. Antibodies and reagents were purchased from the following commercial sources, PX-12 from Santa Cruz

Correspondence to: Hideyuki Kinoshita, Department of Orthopedic Surgery, Chiba Cancer Center, 666-2 Nitonacho, Chuo-ku, Chiba 260-8717, Japan. Tel: +81 432645431, Fax: +81 432628680, e-mail: kinoshi1783@yahoo.co.jp

Key Words: Osteosarcoma, thioredoxin, PX-12, oxidative stress.

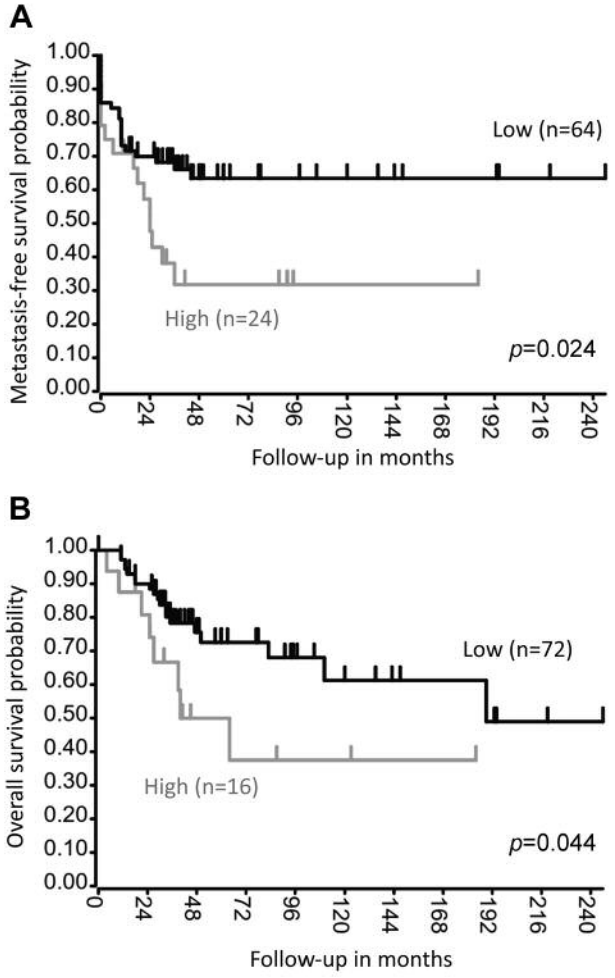

Figure 1. *High-level TXN expression is a negative prognostic factor for metastasis and overall survival in osteosarcoma patients. (A and B) Kaplan–Meier analysis performed on published array data from 2 independent tumor sets [R2: Genomics Analysis and Visualization Platform (http://r2.amc.nl)]. TXN: gene encoding the Trx protein.*

Biotechnology (Santa Cruz, CA, USA); N-Acetyl-L-cysteine (NAC) from Sigma-Aldrich (St. Louis, MO, USA); carbobenzoxy-valyl-alanyl-aspartyl-[O-methyl]- fluoromethylketone (Z-VAD-FMK) from Adooq bioscience (Tokyo, Japan); MEM from Sigma-Aldrich; radioimmunoprecipitation acid (RIPA) lysis buffer from Santa Cruz Biotechnology; anti-Trx-1 (#2429), anti-p38 MAPK (#9212), anti-JNK MAPK (#9252), anti-phospho-p38 MAPK (Thr180/Tyr182) (#9211), anti-phospho-JNK MAPK (Thr183/ Tyr185) (#9251), anti-beta-actin (#4967), and cleaved caspase-3 (Asp175) (#9661) from Cell Signaling Technology (Danvers, MA, USA); horseradish peroxidase-conjugated secondary antibodies and polyvinylidene difluoride (PVDF) western blotting membrane from GE Healthcare (Tokyo, Japan).

Cell culture. The LM8 cell line (RRID: CVCL_6669) was purchased from the RIKEN BioResource Center (Ibaraki, Japan). The cells were maintained in MEM supplemented with 10% fetal

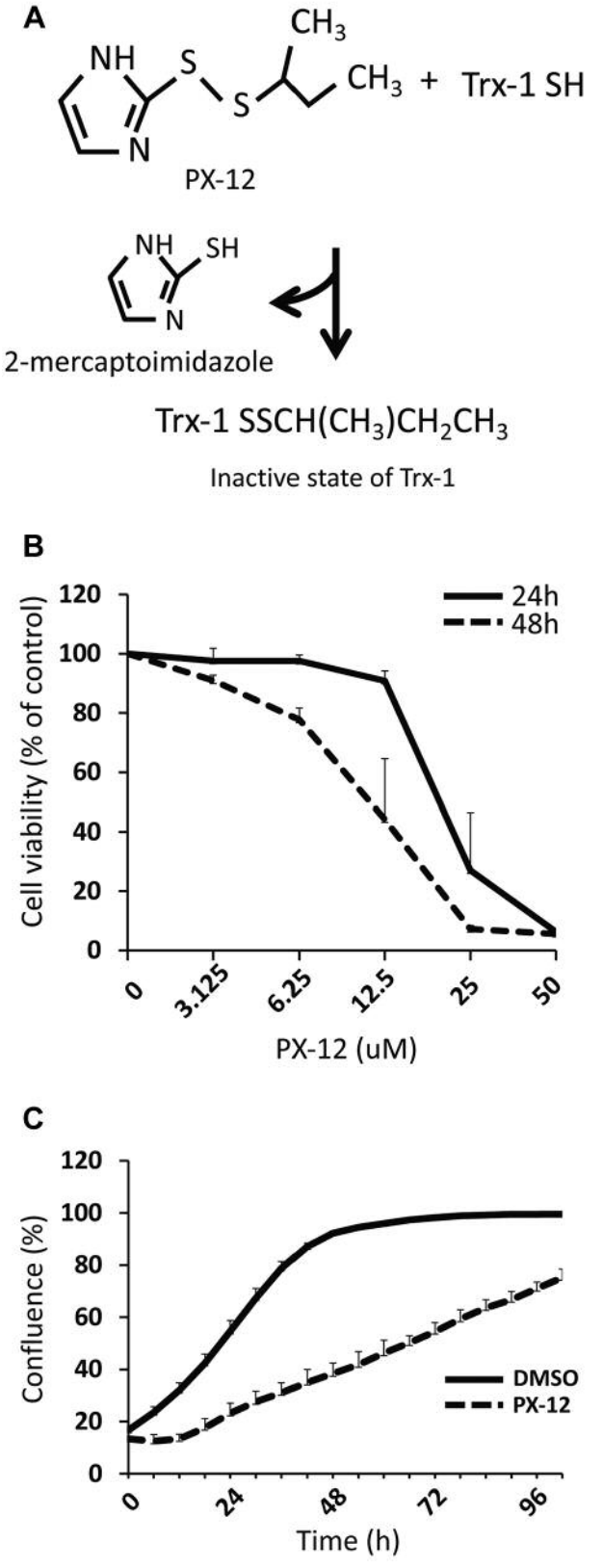

Figure 2. *Continued*

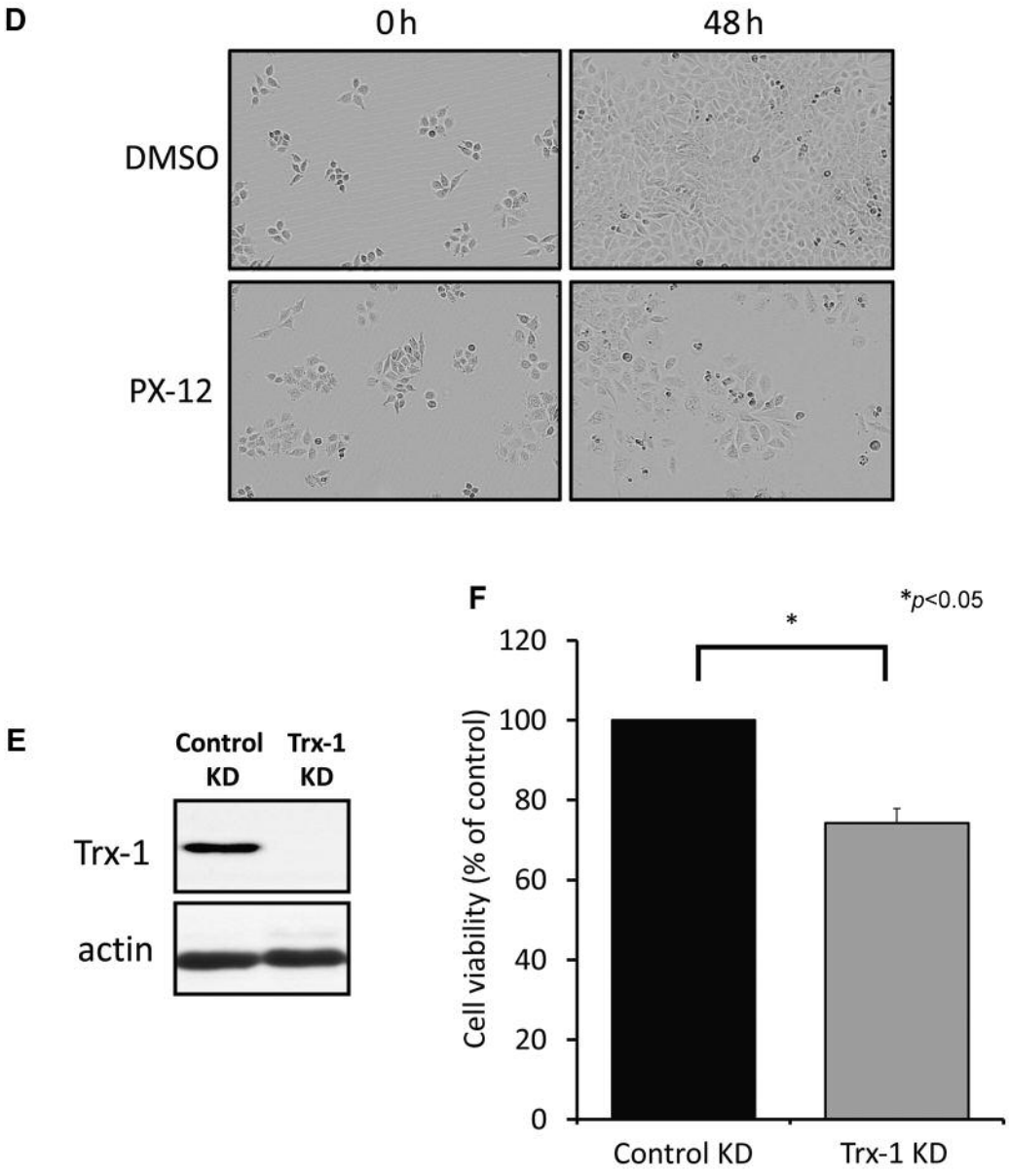

Figure 2. *Effects of PX-12 on LM8 cell proliferation. (A) Schematic diagram of the interaction between PX-12 and Trx-1. (B) PX-12 induced osteosarcoma cell death in a dose- and time-dependent manner. (C) Low-dose PX-12 (5 μM) inhibited LM8 cell growth in a cell proliferation assay. (D) LM8 cell proliferation rate at 0 and 48 h. (E) SiRNA-induced Trx-1 knockdown significantly suppressed Trx-1 protein expression. (F) As compared to the control KD, Trx-1 knockdown in LM8 cells resulted in the suppression of cell proliferation at 48 h.*

bovine serum (FBS) and 100 mg/ml penicillin/streptomycin in a humidified 5% CO_2 atmosphere at 37˚C.

Cell viability assay. LM-8 cells were seeded at a concentration of 1×10^6 cells/ml in a 96-well plate and stimulated with PX-12 (3.125, 6.25, 12.5, 25, and 50 μM) or dimethyl sulfoxide (DMSO) for 24 and 48 h. Subsequently, a 3-(4,5-dimethylthiazol-2-yl)-2,5-diphenyltetrazolium bromide solution (Cayman Chemical, Ann Arbor, MI, USA) was added to the cells at a volume equivalent to 10% of the culture volume under sterile conditions and incubated for 4 h in a 5% CO_2 incubator at 37˚C. After incubation, a crystal-dissolving solution was added to the cultures and incubated for 4-18 h in a CO_2 incubator at 37˚C. The absorbance of each sample at 570 nm was measured using a microplate reader (Multiskan Sky, Thermo Scientific, Tokyo, Japan). Cell viability (%) was calculated based on the following equation: (absorbance value for the experimental group/absorbance value for the control group) × 100.

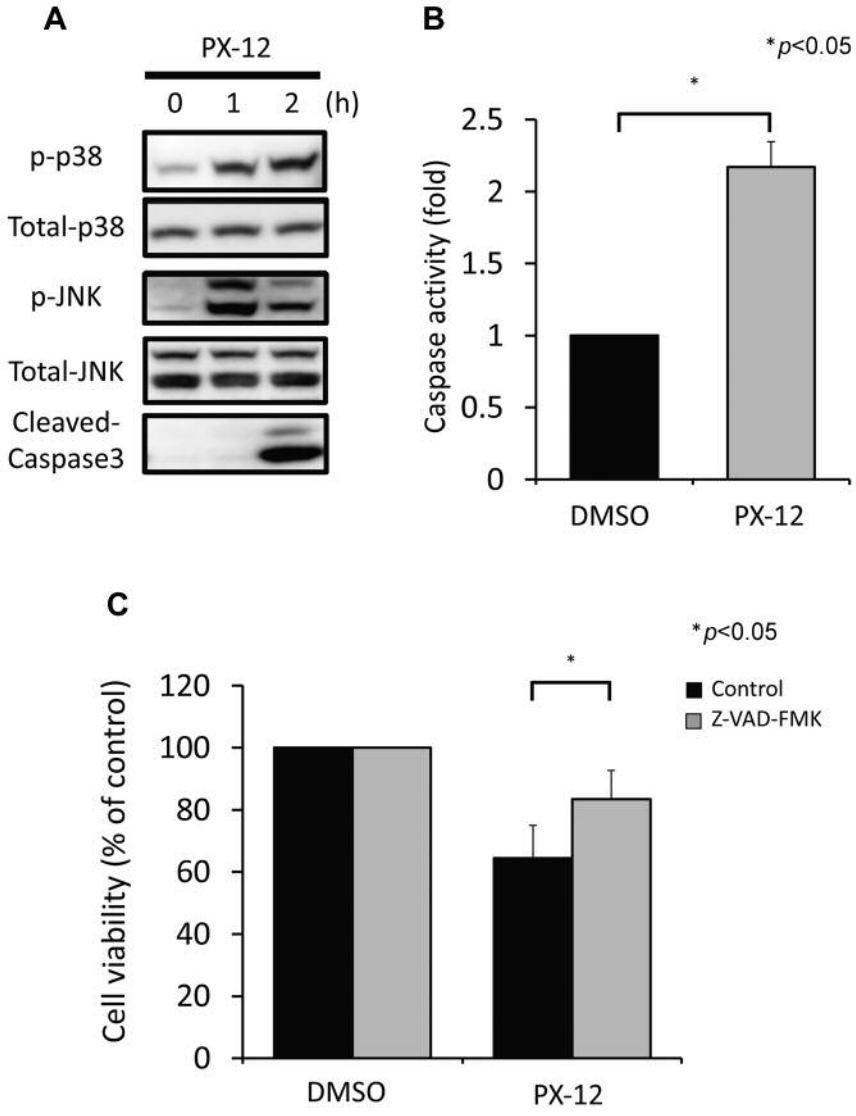

Figure 3. *PX-12 induced apoptosis in OS cells via the MAPK-Caspase 3 pathway. (A) PX-12 (100 μM) induced p38 and JNK phosphorylation and activation, and caspase 3 cleavage in LM8 cells. (B) Caspase assays indicated that PX-12 treatment (50 μM) induced a two-fold increase in caspase activity in the treated group as compared to the control group. *p<0.05 (n=3). (C) Z-VAD-FMK, a pan-caspase inhibitor, significantly reversed PX-12 (20 μM)-induced LM8 cell death. *p<0.05 (n=3). JNK: c-Jun N-terminal kinase; Z-VAD-FMK: carbobenzoxy-valyl-alanyl-aspartyl-[O-methyl]- fluoromethylketone.*

IncuCyte® cell proliferation assay. Cell proliferation was monitored for 96 h using the IncuCyte® ZOOM system (Essen Bioscience, Ann Arbor, MI, USA), which uses an automated incubator to monitor live cells. Growth curves were generated using the algorithm in the ZOOM software and data points were acquired through six-hour-interval imaging. All samples were plated in quadruplicate.

RNA interference. For RNA interference, cells at 60% confluence were transfected with small interfering RNAs (siRNAs) (Life Technologies, Carlsbad, CA, USA) using the Lipofectamine RNAiMAX reagent (Life Technologies) according to the manufacturer's instructions. Then, the cells were transfected with silencer siRNA targeting *TXN* (Catalog #4390824) and silencer select negative control siRNA. After knockdown with each siRNA for 48 h, siRNA-transfected cells were evaluated for cell viability or lysed for immunoblotting.

Immunoblotting. All wash buffers and extraction buffers contained a protease inhibitor cocktail (Roche, Tokyo, Japan), NaF (1 M), the PhosSTOP phosphatase inhibitor (Roche), and Na_3VO_4 (50 μM). Cell extracts were separated using sodium dodecyl sulfate-polyacrylamide gel electrophoresis and electroblotted onto polyvinylidene fluoride membranes. After the membranes were

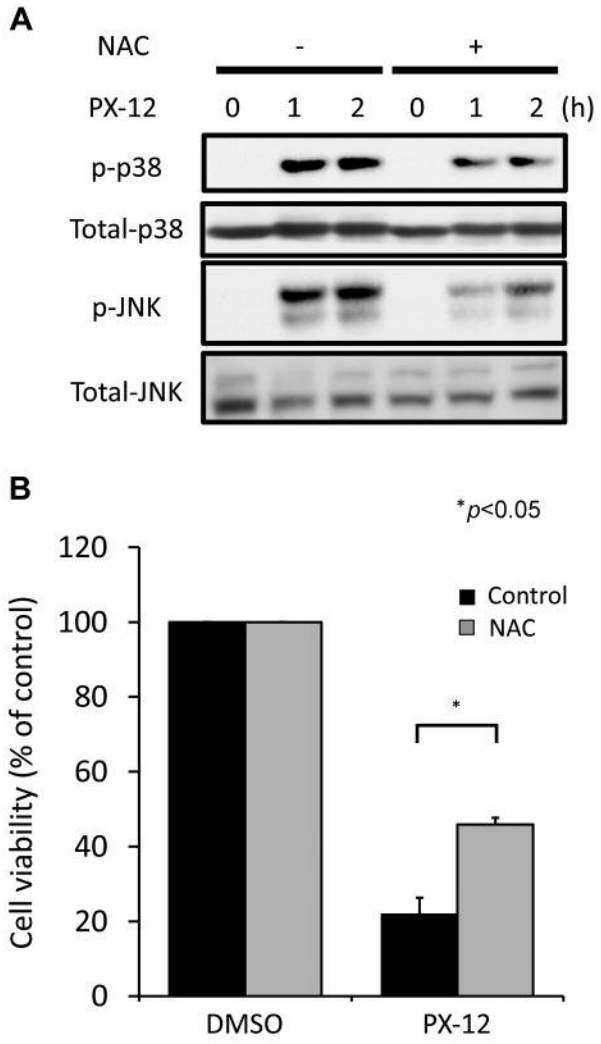

Figure 4. *PX-12 induced apoptosis in OS cells via the oxidative stress-MAPK pathway. (A) Cell pre-treatment with 1 mM NAC, an antioxidant, for 1 h inhibited PX-12 (100 μM)-induced activation of mitogen-activated protein kinases. (B) NAC (1 mM) significantly inhibited PX-12 (20 μM)-induced LM-8 cell death. *p<0.05 (n=3). NAC: N-Acetyl-L-cysteine.*

blocked with 2% bovine serum albumin in TBS-T (150 mM NaCl, 50 mM Tris HCl [pH 8.0], and 0.05% Tween-20), they were probed with antibodies. Antibody-antigen complexes were detected using an enhanced chemiluminescence system (GE Healthcare).

Caspase assay. DMSO- or PX-12-stimulated cells were lysed using a protease inhibitor-free RIPA lysis buffer. A substrate solution was prepared and mixed with phosphate-buffered saline (PBS), 2× reaction buffer (MBL, Tokyo, Japan), and fluorogenic caspase-3 substrate VII Calbiochem, Darmstadt, Germany). The supernatant of the cell solution was mixed with the substrate solution in the wells of a 96-well plate. The plates were incubated at 37˚C for 2 h in the dark, and absorbance was measured using a microplate reader (Multiskan Sky, Thermo Scientific, Tokyo, Japan).

Wound healing assay. Cells were seeded in 6-well plates and cultured until a confluent monolayer was formed. A wound was created in the cell monolayer by scratching the plate with a sterile pipette tip, and the cells were washed with PBS. Then, the cells were pre-treated with 10 μg/ml mitomycin C (Abcam, Tokyo, Japan) at 37˚C for 1 h to inhibit cell proliferation. Next, LM8 cells were incubated with DMSO or PX-12 (10 μM) in 10% FBS for 24 h. Finally, the cells were photographed at a magnification of ×100, 0, 12, and 24 h after incubation. The cell migration distance was measured between the 2 boundaries of the acellular area. The results obtained in the different treatment groups were expressed as the ratio of the original distance.

Animal studies. Five-week-old female C3H/HeSlc mice were purchased from Japan SLC (Shizuoka, Japan). The mice were maintained at a constant temperature (22±2˚C) and humidity (50±10%) under a 12h light/12h dark cycle. All animal experiments were approved by the institutional animal care and use committee of the Chiba cancer center, Chiba, Japan, and were conducted in accordance with institutional guidelines. On day 0, 1×10^7 LM8 cells in 300 μl PBS were subcutaneously injected into the backs of 12 syngeneic C3H/HeSlc mice. Primary tumor growth was allowed to proceed for 7 days prior to treatment until it reached a measurable size (measured using a caliper and determined as length × width^2/2). The mice were then assigned to 2 groups of six mice each with similar tumor size distributions. The mice were treated with either 200 μl of vehicle control (40% polyethylene glycol 300+60% sterile PBS) or 12.5 mg/kg PX-12. Injections were administered when palpable tumors (100-150 mm^3) were observed, and were provided intraperitoneally every other day till the end of the study. Tumor size measurements and animal weights were recorded once a week in a non-blinded manner. On day 35, the mice were euthanized under anesthesia, and the tumors were resected for tumor weight measurement.

Statistical analysis. Experimental data are expressed as the mean±standard deviation. The significance of differences between mean values was determined using Student's *t*-test, with values of $p<0.05$ considered significant. All analyses were performed with SAS software, version 14.2 (SAS Institute, Inc.; Cary, NC, USA).

Results

High-level TXN expression is a negative prognostic factor for metastasis and overall survival in OS patients. Using publicly available expression cohort data, we evaluated *TXN* expression and its correlation with metastasis-free and overall survival in OS patients (Figure 1A and B). High *TXN* expression was correlated with poor metastasis-free and overall survival in the expression cohorts analyzed, suggesting that *TXN* may be a therapeutic target for treating OS progression and metastasis.

The Trx-1 inhibitor, PX-12, induced apoptosis in OS cells via the oxidative stress-MAPK-Caspase 3 pathway. Figure 2A shows a potential schematic for PX-12 metabolism in humans. PX-12 interaction with reduced thiol groups on Trx-1 resulted in the release of 2-mercaptoimidazole- and a thio-

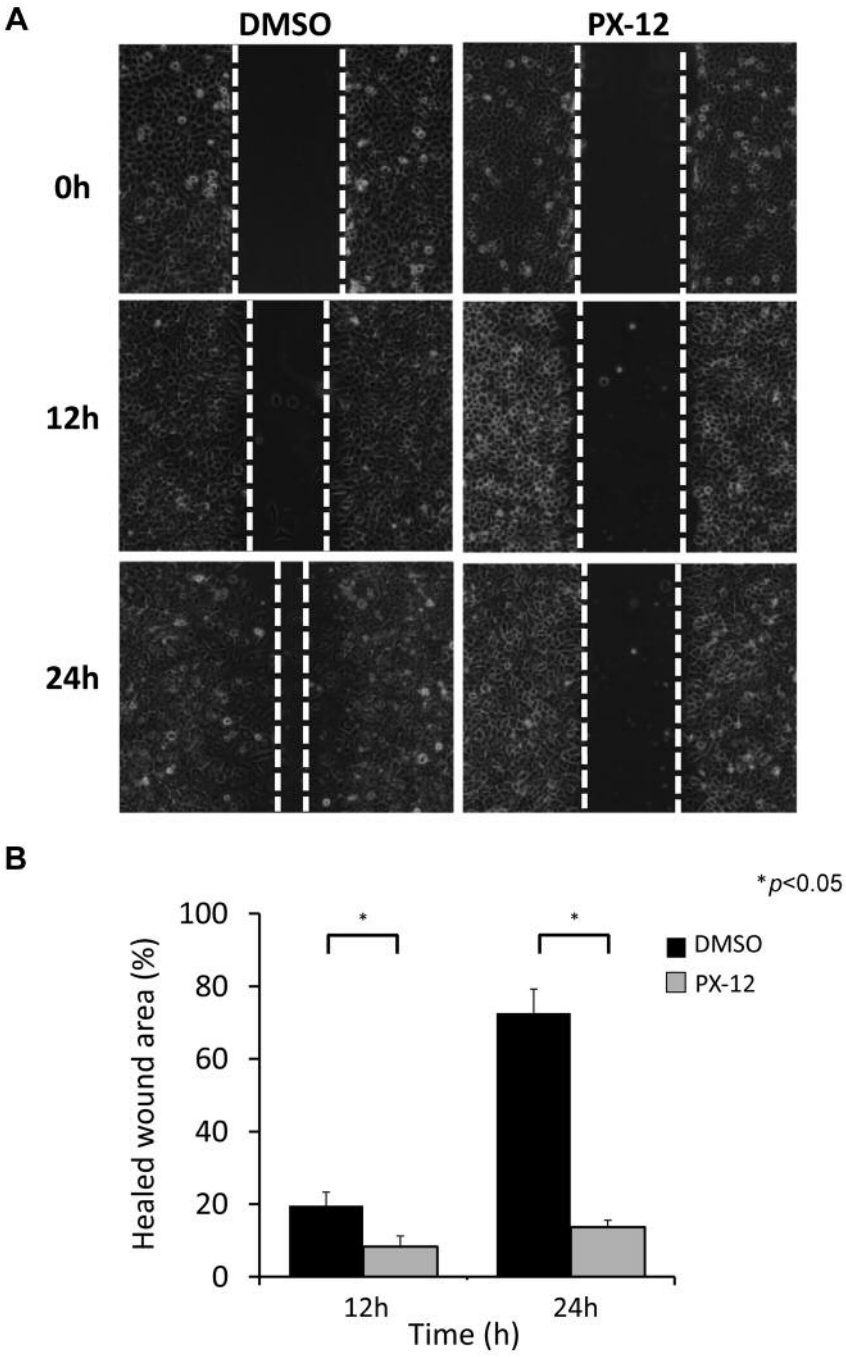

Figure 5. *PX-12 inhibited OS cell migration. (A) PX-12 (10 μM) inhibited LM8 cell migration in the wound healing assay in a time-dependent manner at 12 and 24 h. (B) Significant differences in the calculated healed wound area were observed between DMSO- and PX-12-treated cells; *p<0.05 (n=3). DMSO: Dimethyl sulphoxide.*

alkylated Trx-1, which are its inactive forms. First, we evaluated the effects of PX-12 on LM8 cell proliferation. PX-12 induced cell death in LM8 cells in a dose- and time-dependent manner (Figure 2B). Furthermore, as shown by the findings of the cell proliferation assay, low-dose PX-12 inhibited growth in LM8 cells (Figure 2C and D). As shown by western blotting, siRNA-induced Trx-1 knockdown (KD) significantly suppressed the expression of the Trx-1 protein (Figure 2E). As compared to the control KD, Trx-1 KD in LM8 cells resulted in the suppression of LM8 proliferation

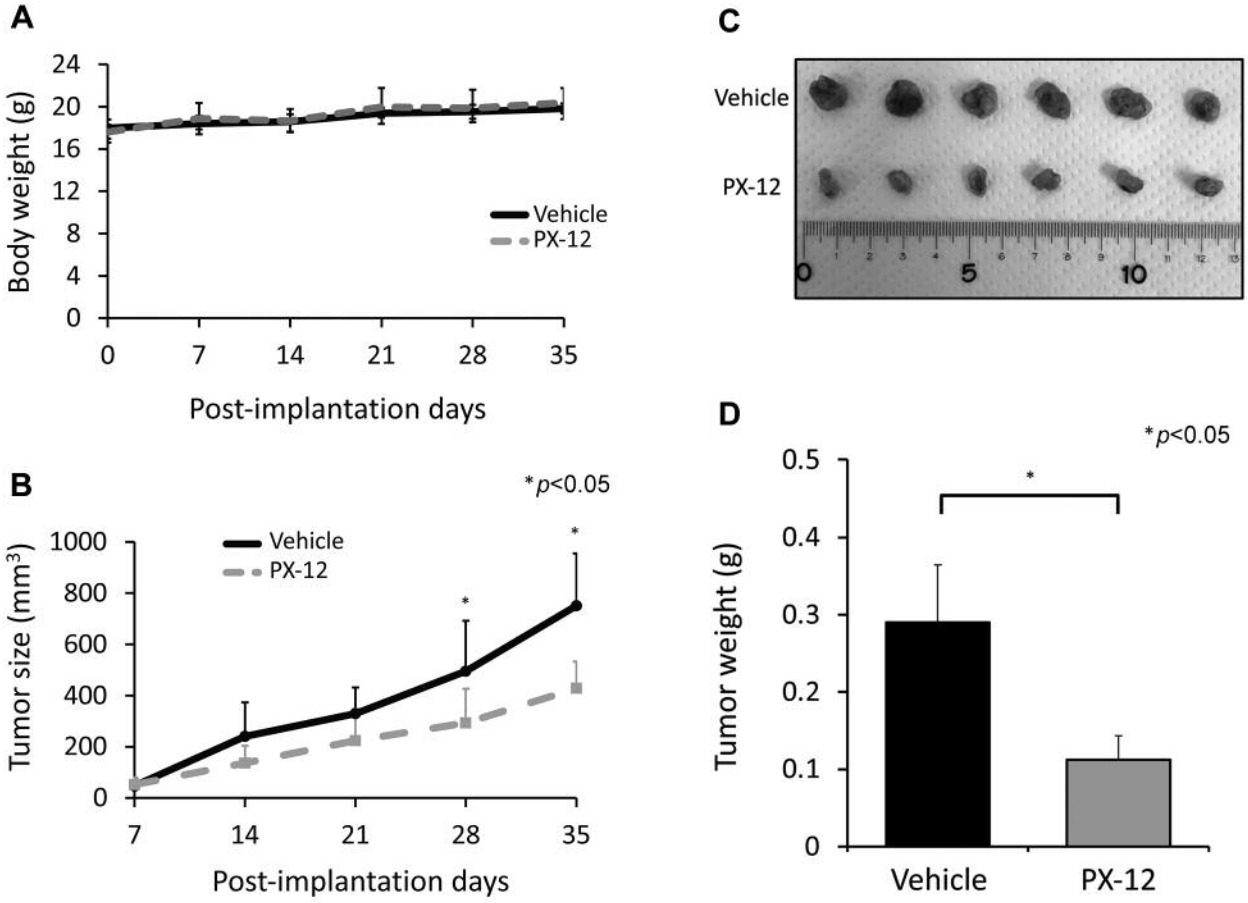

Figure 6. *PX-12 inhibited local OS progression. (A) There was no significant difference in body weight between vehicle- and PX-12-treated mice throughout the course of the study. (B) Based on the evaluation of tumor volume, PX-12 was found to significantly suppress OS tumor progression over time. (C) PX-12 significantly decreased tumor size. (D) PX-12 significantly decreased tumor weight at the time of resection.*

(Figure 2F). Western blot analysis revealed that PX-12 induced p38 and JNK phosphorylation and caspase 3 cleavage, suggesting that it induced apoptosis in LM8 cells (Figure 3A). The findings of the caspase assays indicated that PX-12 induced a two-fold increase in caspase activity in the treatment group as compared to the control group (Figure 3B). Furthermore, Z-VAD-FMK, a pan-caspase inhibitor, significantly reversed PX-12-induced LM8 cell death (Figure 3C). NAC, which is an antioxidant and a precursor of glutathione, was found to inhibit MAPK protein activation by PX-12 (Figure 4A). Moreover, NAC significantly inhibited PX-12-induced LM-8 cell death (Figure 4B), suggesting that PX-12 might have induced cell death *via* the oxidative stress-MAPK-caspase 3 pathway.

PX-12 suppressed OS cell migration. The inhibitory effects of PX-12 on LM8 cell migration were investigated using wound healing assays. PX-12 treatment attenuated the time-dependent LM8 cell migration (Figure 5A). There was a significant difference in the calculated healed wound area between cells treated with DMSO and PX-12 (Figure 5B).

PX-12 inhibited local OS progression. The effects of PX-12 on local OS progression were evaluated in a mouse model. There was no significant difference in body weight between mice in the vehicle and PX-12 groups throughout the course of the study (Figure 6A). Based on the evaluation of tumor volume, PX-12 was found to significantly suppress OS tumor progression over time (Figure 6B). Furthermore, PX-12 significantly suppressed tumor size and weight at the time of excision (Figure 6C and D).

Discussion

In this study, through bioinformatics analyses, we found that *TXN* may be a negative prognostic factor for metastasis and

overall survival in OS patients. The findings of *in vitro* assays indicated that PX-12 induced apoptosis *via* the oxidative stress-MAPK-caspase 3 pathway and further suppressed OS cell migration. Furthermore, PX-12 significantly inhibited local OS progression *in vivo*.

The redox system, which includes Trx and TrxR, has been found to be associated with the local progression and metastasis of several cancers (7, 8). A redox imbalance induces oxidative stress, which leads to cancer cell death. Many anticancer drugs induce oxidative stress in cancer cells (9). Samaranayake *et al*. reported that Trx-1 protects cells against androgen receptor-induced redox vulnerability in castration-resistant prostate cancer, suggesting that Trx-1 inhibitors could be potential therapeutic agents for progressive prostate cancer treatment (10). Many studies have reported that PX-12 is effective in treating various cancers; it induces mitochondria-mediated apoptosis in acute lymphoblastic leukemia cells (11). Furthermore, Shang *et al*. reported that Trx-1 knockdown suppresses cell proliferation, migration, and invasion in gastric cancer cells *in vitro* and suppresses tumor growth and lung metastasis *in vivo* (12). In addition, colorectal cancer cell migration and invasion were found to be inhibited by low dose PX-12 (13). In the current study, high *TXN* expression was found to be correlated with poor metastasis-free survival in the expression cohorts, and PX-12 was efficacious in suppressing OS cell migration *in vitro*. However, although PX-12 inhibited local OS progression *in vivo*, its inhibitory effects on OS lung metastasis were not confirmed (data not shown). Whether or not the inability of PX-12 to inhibit lung metastasis was due to the volume administered or the method of administration is unclear, and needs to be clarified in the future.

Clinical studies have also confirmed the anticancer effects of PX-12 (14). Ramesh *et al*. investigated the tolerability, safety, pharmacokinetics, and pharmacodynamics of PX-12 in advanced solid tumors, including pancreatic cancer (15). However, due to unexpectedly low baseline plasma Trx-1 levels and the lack of significant antitumor activity, the study was discontinued (16). In the current study, low PX-12 doses were found to be less effective in preventing local OS progression; however, when it was administered daily, it induced significant weakness in the mice. Since Li *et al*. reported that PX-12 exhibits anti-tumor activity and that it has synergistic effects with 5-FU against hepatocellular carcinoma (17), it may be plausible to explore the effects PX-12 in combination with other drugs against OS. PX-12 may have a narrow therapeutic window, and further basic and clinical research is necessary to validate its clinical application.

Recently, we reported that AUR, which is a TrxR inhibitor, significantly inhibits pulmonary OS metastasis *in vivo* (4). In addition, considering the fact that PX-12 significantly inhibited local OS progression, the redox system may be a potential therapeutic target for osteosarcoma treatment. However, this study has several limitations. First, we could not precisely evaluate the possible efficacy of PX-12 in inhibiting OS lung metastasis. Second, only murine cell lines and mouse models were tested in this study; thus, it is necessary to use patient-derived xenografts in future studies.

Conclusion

We found that PX-12 significantly inhibits local OS progression *in vitro* and *in vivo*. However, further studies that will evaluate the possible efficacy of PX-12 in inhibiting OS lung metastasis are needed. Furthermore, a study that will be based on patient-derived xenografts and not on LM8-implanted murine models is desirable in the future.

Conflicts of Interest

The Authors have no conflicts of interest directly relevant to the content of this article.

Authors' Contributions

H.K designed and performed experiments, analyzed data and wrote the article; O.S, T.I, H.K, Y.H, S.O and T.Y provided technical support and conceptual advice.

Acknowledgements

This work was supported by JSPS KAKENHI grants (19K16760), Cancer Research Funds for Patients and Family, Foundation for Promotion of Cancer Research in Japan, Funds for Inohana Shougakukai, Funds for Children's Cancer Association of Japan, Funds for Gold Ribbon Network and Kawano Masanori Memorial Public Interest Incorporated Foundation for Promotion of Pediatrics.

References

1 Kinoshita H, Yonemoto T, Kamoda H, Hagiwara Y, Tsukanishi T, Inoue M, Terakawa F, Ohtori S and Ishii T: Effectiveness of salvage knee rotationplasty on sarcoma around the knee in adolescents and young adults. Anticancer Res *41(2)*: 1041-1046, 2021. PMID: 33517313. DOI: 10.21873/anticanres.14860

2 Yang M, Zhang W, Yu X, Wang F, Li Y, Zhang Y and Yang Y: Helenalin facilitates reactive oxygen species-mediated apoptosis and cell cycle arrest by targeting thioredoxin reductase-1 in human prostate cancer cells. Med Sci Monit *27*: e930083, 2021. PMID: 34125740. DOI: 10.12659/MSM.930083

3 Al-Khayal K, Vaali-Mohammed MA, Elwatidy M, Bin Traiki T, Al-Obeed O, Azam M, Khan Z, Abdulla M and Ahmad R: A novel coordination complex of platinum (PT) induces cell death in colorectal cancer by altering redox balance and modulating MAPK pathway. BMC Cancer *20(1)*: 685, 2020. PMID: 32703189. DOI: 10.1186/s12885-020-07165-w

4 Kinoshita H, Shimozato O, Ishii T, Kamoda H, Hagiwara Y, Tsukanishi T, Ohtori S and Yonemoto T: The thioredoxin reductase inhibitor auranofin suppresses pulmonary metastasis of

osteosarcoma, but not local progression. Anticancer Res *41(10)*: 4947-4955, 2021. PMID: 34593442. DOI: 10.21873/anticanres.15308

5 Samaranayake GJ, Troccoli CI, Huynh M, Lyles RDZ, Kage K, Win A, Lakshmanan V, Kwon D, Ban Y, Chen SX, Zarco ER, Jorda M, Burnstein KL and Rai P: Thioredoxin-1 protects against androgen receptor-induced redox vulnerability in castration-resistant prostate cancer. Nat Commun *8(1)*: 1204, 2017. PMID: 29089489. DOI: 10.1038/s41467-017-01269-x

6 Flores LC, Roman MG, Cunningham GM, Cheng C, Dube S, Allen C, Van Remmen H, Hubbard GB, Saunders TL and Ikeno Y: Continuous overexpression of thioredoxin 1 enhances cancer development and does not extend maximum lifespan in male C57BL/6 mice. Pathobiol Aging Age Relat Dis *8(1)*: 1533754, 2018. PMID: 30370017. DOI: 10.1080/20010001.2018.1533754

7 Qayyum N, Haseeb M, Kim MS and Choi S: Role of thioredoxin-interacting protein in diseases and its therapeutic outlook. Int J Mol Sci *22(5)*: 2754, 2021. PMID: 33803178. DOI: 10.3390/ijms22052754

8 Zhang J, Duan D, Osama A and Fang J: Natural molecules targeting thioredoxin system and their therapeutic potential. Antioxid Redox Signal *34(14)*: 1083-1107, 2021. PMID: 33115246. DOI: 10.1089/ars.2020.8213

9 Lincoln DT, Ali Emadi EM, Tonissen KF and Clarke FM: The thioredoxin-thioredoxin reductase system: over-expression in human cancer. Anticancer Res *23(3B)*: 2425-2433, 2003. PMID: 12894524.

10 Samaranayake GJ, Troccoli CI, Huynh M, Lyles RDZ, Kage K, Win A, Lakshmanan V, Kwon D, Ban Y, Chen SX, Zarco ER, Jorda M, Burnstein KL and Rai P: Thioredoxin-1 protects against androgen receptor-induced redox vulnerability in castration-resistant prostate cancer. Nat Commun *8(1)*: 1204, 2017. PMID: 29089489. DOI: 10.1038/s41467-017-01269-x

11 Ehrenfeld V and Fulda S: Thioredoxin inhibitor PX-12 induces mitochondria-mediated apoptosis in acute lymphoblastic leukemia cells. Biol Chem *401(2)*: 273-283, 2020. PMID: 31352431. DOI: 10.1515/hsz-2019-0160

12 Shang W, Xie Z, Lu F, Fang D, Tang T, Bi R, Chen L and Jiang L: Increased thioredoxin-1 expression promotes cancer progression and predicts poor prognosis in patients with gastric cancer. Oxid Med Cell Longev *2019*: 9291683, 2019. PMID: 30911354. DOI: 10.1155/2019/9291683

13 Wang F, Lin F, Zhang P, Ni W, Bi L, Wu J and Jiang L: Thioredoxin-1 inhibitor, 1-methylpropyl 2-imidazolyl disulfide, inhibits the growth, migration and invasion of colorectal cancer cell lines. Oncol Rep *33(2)*: 967-973, 2015. PMID: 25483731. DOI: 10.3892/or.2014.3652

14 Baker AF, Adab KN, Raghunand N, Chow H, Stratton SP, Squire SW, Boice M, Pestano LA, Kirkpatrick DL and Dragovich T: A phase IB trial of 24-hour intravenous PX-12, a thioredoxin-1 inhibitor, in patients with advanced gastrointestinal cancers. Invest New Drugs *31(3)*: 631-641, 2013. PMID: 22711542. DOI: 10.1007/s10637-012-9846-2

15 Ramanathan RK, Kirkpatrick DL, Belani CP, Friedland D, Green SB, Chow HH, Cordova CA, Stratton SP, Sharlow ER, Baker A and Dragovich T: A Phase I pharmacokinetic and pharmacodynamic study of PX-12, a novel inhibitor of thioredoxin-1, in patients with advanced solid tumors. Clin Cancer Res *13(7)*: 2109-2114, 2007. PMID: 17404093. DOI: 10.1158/1078-0432.CCR-06-2250

16 Ramanathan RK, Abbruzzese J, Dragovich T, Kirkpatrick L, Guillen JM, Baker AF, Pestano LA, Green S and Von Hoff DD: A randomized phase II study of PX-12, an inhibitor of thioredoxin in patients with advanced cancer of the pancreas following progression after a gemcitabine-containing combination. Cancer Chemother Pharmacol *67(3)*: 503-509, 2011. PMID: 20461382. DOI: 10.1007/s00280-010-1343-8

17 Li GZ, Liang HF, Liao B, Zhang L, Ni YA, Zhou HH, Zhang EL, Zhang BX and Chen XP: PX-12 inhibits the growth of hepatocelluar carcinoma by inducing S-phase arrest, ROS-dependent apoptosis and enhances 5-FU cytotoxicity. Am J Transl Res *7(9)*: 1528-1540, 2015. PMID: 26550453.

Received October 2, 2021
Revised October 30, 2021
Accepted November 1, 2021